

A response analysis with effective stress model by using vertical input motions

H.Yamanouchi & I.Ohkawa
Building Research Institute, Tsukuba, Japan
O.Chiba, M.Tohdo & O.Kaneko
Toda Construction Co., Ltd, Tokyo, Japan

1 INTRODUCTION

The nuclear power plant reactor buildings are to be directly supported on a hard soil as a rule in Japan. In case of determining the input motions in order to design those buildings; the amplifications of the hard soil deposits are examined by the total stress analysis in general.

However, when the supporting hard soil is replaced with the slightly softer medium such as sandy or gravelly soil, the existence of pore water, in other words, the contribution of the pore water pressure to the total stress cannot be ignored even in a practical sense.

In this paper we defined an analytical model considering the effective stress-strain relation. In the analyses, the response in the vertical direction is used to evaluate the confining pressure, at first. In the next step, the process of the generation and dissipation of the pore water pressure is taken into account, together with the effect of the confining pressure. We applied these procedures for the response computations of the horizontally layered soil deposits.

2 EVALUATION OF EFFECTIVE SHEAR STRESS

The Ramberg-Osgood model (hereafter abbreviated as R-O model) is widely used to express the stress-strain relation of soils. This model is also used in the present analyses.

2.1 Stress-strain relation and hysteresis rule

The R-O model is expressed as,

$$\gamma = \frac{\tau}{G_0} (1 + \alpha |\tau|^\beta), \quad \alpha = \left(\frac{2}{\gamma_{0.5} G_0} \right)^\beta, \quad \beta = \frac{2\pi h_{\max}}{2 - \pi h_{\max}}$$

Since G_0 , α are the functions of effective stress, the following transforms of parameters are made, (Iwasaki, et al., 1978, Shibata, et al., 1978)

$$G_0^* = G_0 R_s^m, \quad \alpha^* = \alpha R_s^{-n}, \quad R_s = \sigma_v' / \sigma_{v0}'$$

where $\gamma_{0.5}$ is the shear strain when $G/G_0 = 0.5$, G_0 is the initial shear modulus, σ_v' is the effective overburden pressure, and h_{\max} is the

maximum damping ratio. The parameters m and n are constants derived from the test results. When these expressions are substituted into the above equation, the relation becomes an identical expression with the original one except the meaning of each parameter.

where,

$$\gamma^* = \frac{\tau^*}{G_0} (1 + \alpha |\tau^*|^\beta)$$

$$\gamma^* = \gamma R_s \frac{m-n}{\beta}, \quad \tau^* = \tau R_s \frac{n}{\beta}$$

The hysteresis rule follows the Masing's law. The above equation is used as the skeleton curve of the hysteresis curve.

2.2 Generation of pore water pressure

In the analysis, the pore water pressure (hereafter abbreviated as PWP) is evaluated from the relation between the cyclic shear stress ratio: τ/σ'_v obtained from the laboratory test and the cyclic number of shear stress necessary to cause liquefaction: N_1 and the relation between PWP ratio $\Delta U/\sigma'_v$ and the cyclic ratio N/N_1 . (ΔU :excess PWP)

The relation between τ/σ'_v and N_1 is assumed to be bi-linear on a full-log scale as shown in Fig.1(a). This assumption is based on many test results in the past and is generally acceptable.

The procedure to determine the response is as follows;

- (1) Determine the cyclic number $N_1(t=t_i)$ necessary to cause liquefaction, if the cyclic loading with constant amplitude $\tau(t=t_i)$ are continued.
- (2) Determine the equivalent wave number NA during the time interval Δt .
- (3) Determine the cyclic ratio $NA/N_1(t=t_i)$ at the beginning of the time interval ($t=t_i$) from the effective overburden pressure. This can easily be done, since the cyclic number of shear stress at the instant is known. The process is shown in Fig.1(b).
- (4) Determine PWP ratio due to the additional shear stress applied during the step. Here, the change in confining pressure σ'_v is evaluated from the vertical response.

The following relation between PWP ratio $\Delta U/\sigma'_v$ and cycle ratio N/N_1 is employed. (Seed, et al., 1976)

$$\Delta U/\sigma'_v = \frac{2}{\pi} \sin^{-1} \left(\frac{N}{N_1} \right)^{1/2\theta}$$

In this equation, θ is the constant to be determined from the laboratory tests, and it is practically a function of the relative density D_r , τ/σ'_v and N_1 .

2.3 Dissipation of pore water pressure

The dissipation process of PWP is evaluated with the one-dimensional seepage theory in which the following assumptions are adopted. (Seed, et al., 1976)

- i) Water flow follows Darcy's law

$$v = k \cdot i = \frac{k}{\gamma_w} \frac{\partial u}{\partial z}$$

where v is the flow velocity (cm/sec), k is the permeability coefficient (cm/sec), i is the hydraulic gradient, u is the PWP.

- ii) Continuity in flow velocity

$$\partial \epsilon_v / \partial t = \partial v_z / \partial z$$

where ϵ_v is the volume strain. The volume change due to the change in PWP is expressed as follows;

$$d\epsilon = m_v (du - \Delta U), \quad \frac{\partial \epsilon}{\partial t} = m_v \left(\frac{\partial u}{\partial t} - \frac{\Delta U}{\Delta N} \frac{\partial N}{\partial t} \right)$$

where m_v is the coefficient of volume compressibility (cm^2/kg).
Then,

$$\frac{\partial}{\partial z} \left(\frac{k}{\gamma} \frac{\partial u}{\partial z} \right) = m_v \left(\frac{\partial u}{\partial t} - \frac{\Delta U}{\Delta N} \frac{\partial N}{\partial t} \right)$$

The flow chart of the computer program used herein is shown in Fig.2.

3 COMPUTATIONAL RESULTS

The soil profile used in the analyses is shown in Fig.3. The soil deposit consists of clay, medium sand, dense sand from the ground surface, and the shear wave velocity (V_s) of the base layer is 600 m/sec.

The input motion is the recorded motion at Cholame Shandon during the Parkfield earthquake in 1966, the magnitude and the focal depth of which are 5.6 and 9.6 km, respectively. The NS and UD components of the record are used in the analyses. These input motions are treated as the motions of the exposed base layer.

Totally five cases are examined as shown in Table 1. In the cases (1) and (3), Only the horizontal responses are considered. These correspond to the total stress analyses. In the cases (2) and (4), the input motions are simultaneously applied in two directions. The vertical responses are used to evaluate the confining pressures. In the case (5), the confining pressure and generation and dissipation process of PWP are both considered.

For the response computations in vertical direction, the physical constants of each layer are assumed to be same as those for the horizontal direction. The soil medium is assumed to be isotropic.

In Fig.4, the distributions of the maximum response accelerations and the shear strains with depth are shown. As seen from the figures, The difference between the responses are negligibly small, when only the changes in the confining pressure due to the vertical input motions are taken into account. (i.e., comparisons between cases (1) and (2) or cases (3) and (4)). On the other hand, the result of case (5), in which the change in PWP is considered, shows some differences, especially remarkable in the medium dense sand layer. (i.e., the amount of the induced PWP is large) It is also seen that in the medium dense sand layer, the excess PWP is generated and the effective confining pressure is reduced, the acceleration becomes less and the shear strain becomes larger than the other cases owing to the reduction of the shear modulus.

In Fig.5, the stress-strain relations of the medium dense sand are shown for the cases (3), (4) and (5). Also for the case (5), the time history of the effective overburden pressure is shown in Fig.6.

As seen from these figures, it can be said that the confining pressure does not change the horizontal response so much, but the generation and dissipation of PWP decreases the acceleration responses and increases the strain responses of the dense sand layers.

4 CONCLUSIONS

The used model, in which the effective stresses are considered is the expansion of the widely-used R-O type model. The applicability of the R-O model is certified through many laboratory tests and the physical meanings of the parameters appearing in the expressions are rather clearer than those of other models. These parameters can be readily identified by laboratory tests.

The analytical model of the generation and dissipation process of the excess PWP is introduced to evaluate the effective stress. Comparing with the other models, this model is highly empirical and test-dependent, since the dynamic characteristics of sandy soils have not yet been made so clear and it is required to conduct many laboratory tests, although the model itself may be sufficiently lucid.

From the computational results, the earthquake induced vertical input motion does not affect so much on the horizontal response. On the other hand, the change in PWP does greatly. This is due to that the effect of vertical motion is temporary, i.e., the shear modulus restores when the earthquake loading is removed, but the excess PWP is accumulated in the later steps.

The liquefaction phenomenon has been investigated mainly for the loose sand. However, from the view point of aseismic design of the nuclear power plant reactor buildings, it is necessary to introduce the concept of cyclic mobility peculiar to dense sand and gravel for the analyses in the following stages.

REFERENCES

- Iwasaki, T., et al. 1978. Shear moduli of sands under cyclic torsional loading. *Soils and Foundations*. 1:39-56
- Shibata, T., et al. 1978. Stress-strain characteristics of clay under cyclic loading. *Proceedings of Japan Society of Civil Engineers*. 276:101-110 (in Japanese)
- Seed, H. B., et al. 1976. GADFLEA: A computer program for the analysis of pore pressure generation and dissipation during cyclic or earthquake loading. *Earthquake Engineering Research Center Report*. 76-24

Table 1. Five cases of analyses

Case No.	Max. Acceleration (gal) *1		PWP
	horizontal	vertical	
1	200	- *2	-
2	200	100	-
3	400	-	-
4	400	200	-
5	400	200	o

*1 Input time histories are uniformly normalized by the maximum values listed above.

*2 Symbols (o), (-) indicate considered and not considered, respectively.

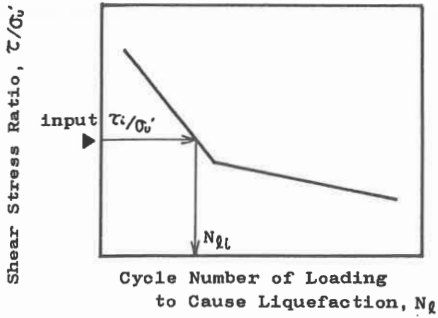


Fig.1(a) The relation between cyclic shear stress ratio and cyclic number of shear stress necessary to cause liquefaction

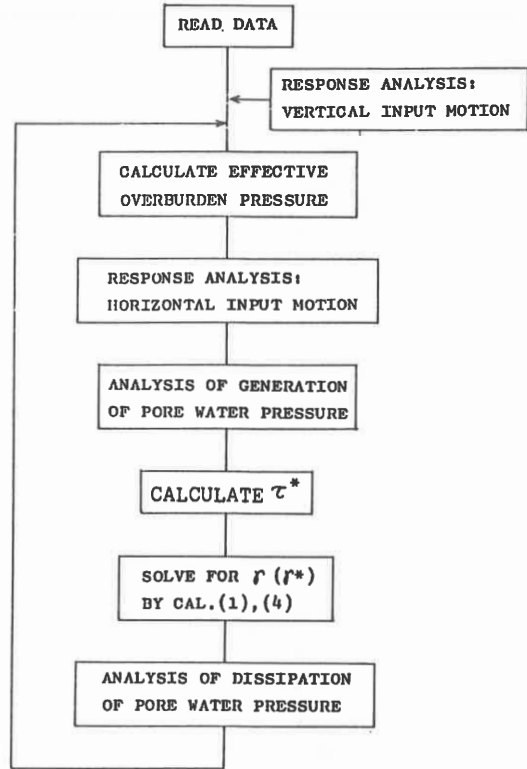


Fig.2 Flow chart for response computations

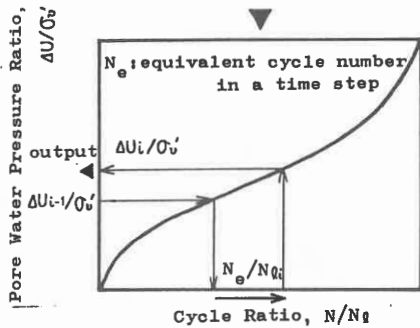
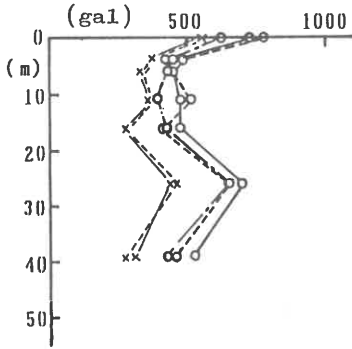


Fig.1(b) Process to determine the pore water pressure ratio

DEPTH (m)	γ_d (t/m^3)	V_s (m/s)	G_0 (kg/cm^2)	k (cm/s)	α	β	m	n
0.0	1.5	80	100	0.000001	11.6	1.29	0.5	0.7
clay	1.6	100	160		6.3			
silt	1.8	120	250		21.3			
20.0	2.0	150	440	0.00001	17.9	1.47	0.75	
sand	1.8	210	810		7.4			
30.0	1.8	400	3000	0.001	1.2	1.78	0.8	
40.0								
50.0								

Fig.3 Physical properties of the soil deposits for the response computations. γ_d : unit weight (t/m^3), V_s : shear wave velocity (m/sec) G_0 : initial shear modulus (kg/cm^2), k : permeability coefficient (cm/sec)

MAXIMUM RESPONSE ACCELERATION



MAXIMUM RESPONSE STRAIN

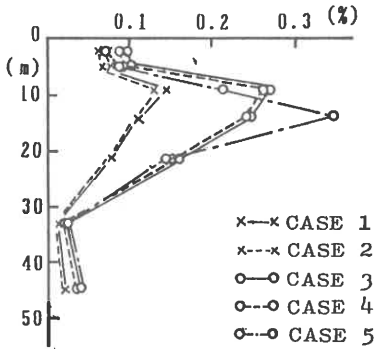


Fig.4 Distributions of the maximum acceleration response (a) and the maximum strain amplitude (b) of each layer with depth

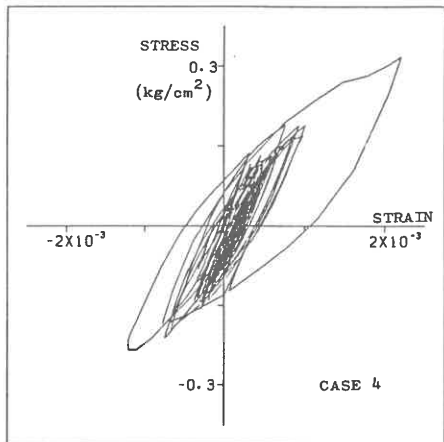
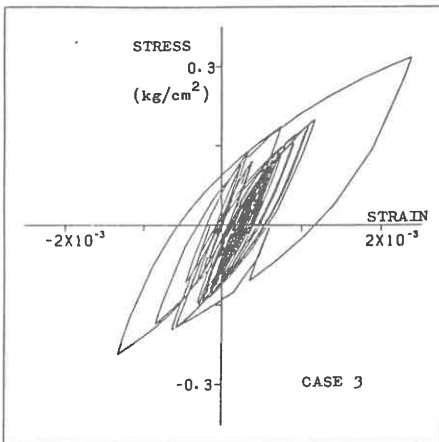


Fig.5(a) The stress-strain relation of medium dense sand for case (3)

Fig.5(b) The stress-strain relation of medium dense sand for case (4)

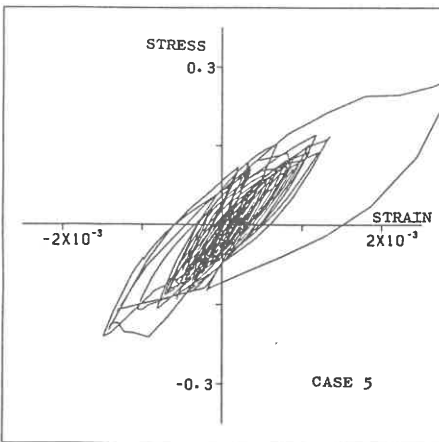


Fig.5(c) The stress-strain relation of medium dense sand for case (5)

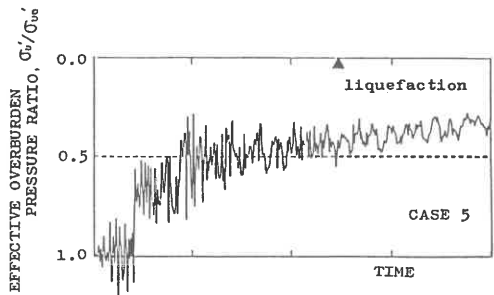


Fig.6 Time history of the effective overburden pressure for medium dense sand layer